Supplement of Atmos. Meas. Tech., 13, 6733–6754, 2020
https://doi.org/10.5194/amt-13-6733-2020-supplement

Atmospheric Measurement Techniques
Open Access

Supplement of

Quantifying CO_2 emissions of a city with the Copernicus Anthropogenic CO_2 Monitoring satellite mission

Gerrit Kuhlmann et al.

Correspondence to: Gerrit Kuhlmann (gerrit.kuhlmann@empa.ch) and Dominik Brunner (dominik.brunner@empa.ch)

S1 Arc length and distance from the center line

For the mass-balance approach, a two-dimensional curve $\boldsymbol{p}(r)$ is fitted that consists of two parabolic polynomials:

$$x(r) = a_0 r^2 + a_1 r + a_2 \tag{1}$$

$$y(r) = b_0 r^2 + b_1 r + b_2 \tag{2}$$

with coefficients a_k and b_k and radial distance r. The parameter is calculated as the distance from the origin

$$r = \sqrt{(x - x_o)^2 + (y - y_o)^2} \tag{3}$$

where x and y are easting and northing in the "DHDN / Soldner Berlin" spatial reference system (EPSG: 3068).

To converts pixel coordinates in easting and northing to plume coordinates, we need to compute the arc length of the curve from the origin of the source x_p and the distance of the pixel center from the curve y_p. The minimum distance can be found by minimizing the following equation

$$\min_r \left[(x(r) - p_x)^2 + (y(r) - p_y)^2 \right] \tag{4}$$

which can be done by substituting $x(r)$ and $y(r)$, taking the first derivative and finding the values for r where the first derivative is equal to zero. The steps were executed using the Sympy Library (www.sympy.org), which is a Python library for symbolic computing. The result is a cubic equation for which the roots can be computed using the general cubic formula (e.g. https://en.wikipedia.org/wiki/Cubic_equation#General_cubic_formula). The shortest distance to the curve was used in case of multiple (real) solutions. The sign for the distance was assigned a negative value if the pixel was on the right side of the curve when viewed from the source location and positive otherwise.

The along-plume distance is the arc length x_p from the source origin to the point where the satellite pixel is perpendicular to the curve. The arc length for a parametric curve (computed from the source origin to the points computed above) is

$$s = \int_a^b \sqrt{\left(\frac{\partial x(r)}{\partial r}\right)^2 + \left(\frac{\partial y(r)}{\partial r}\right)^2} \tag{5}$$

which with Eq. (1) results in the integral over the square root of a quadratic polynomial whose solution can be found in most integral tables (e.g. Eq. (37) on http://integral-table.com/):

$$\int \sqrt{ax^2 + bx + c}\, dx = \frac{b + 2ax}{4a} \sqrt{ax^2 + bx + c} + \frac{4ac - b^2}{8a^{3/2}} \ln \left| 2ax + b + 2\sqrt{a(ax^2 + bx + c)} \right|. \tag{6}$$

S2 Hermite spline

The seasonal cycle is fitted by a cubic Hermite spline with periodic boundary conditions:

$$s(\xi) = p_k \cdot (1 + 2\xi)(1 - \xi)^2 + m_k \cdot \xi(1 - \xi)^2 + p_{k+1} \cdot \xi^2(3 - 2\xi) + m_{k+1} \cdot \xi^2(\xi - 1) \tag{7}$$

with control points p_k and three-point difference m_k.

S3 Additional figures

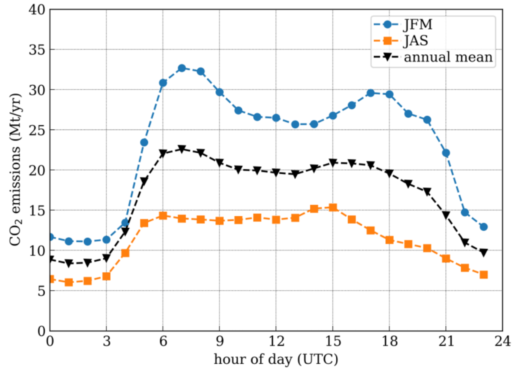

Figure S1. Diurnal cycle of Berlin's CO_2 emissions for winter (JFM: January, February and March) and summer (JAS:July, August and September).

(a)

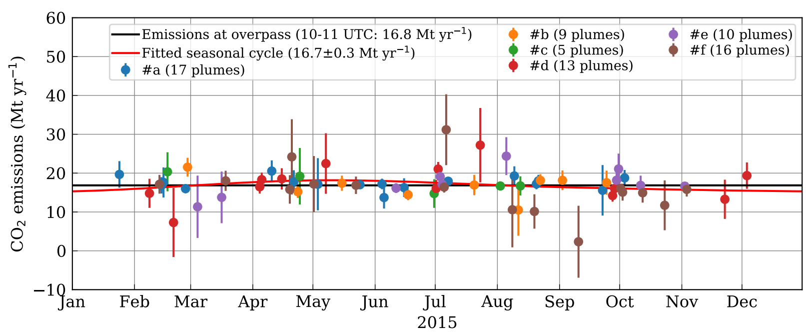

(b)

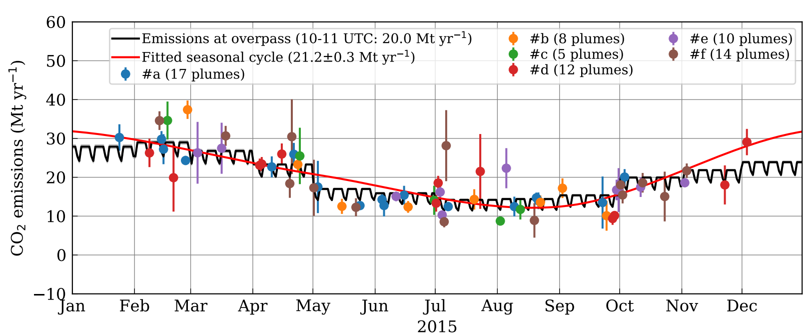

Figure S2. Time series of CO_2 emissions of Berlin estimated with the analytical inversion using six satellites with σ_{VEG50} of 0.7 ppm for (a) constant and (b) time-varying emissions. Emission estimates with uncertainties larger than $10.0\,\mathrm{Mt\,yr^{-1}}$ (50% of mean emissions at 11:30 local time) are not shown.

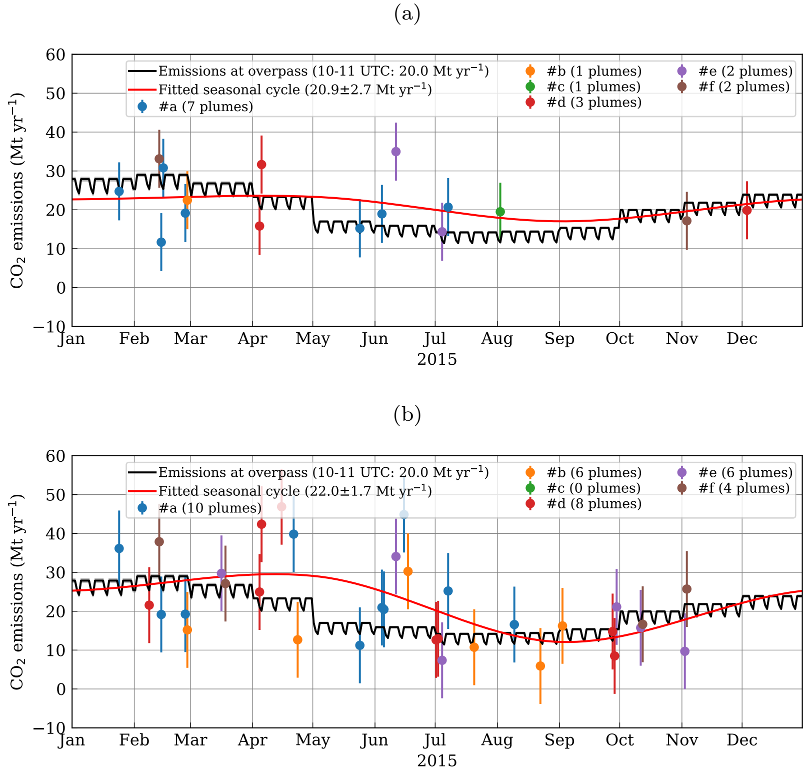

Figure S3. Time series of estimated CO_2 emissions of Berlin using a constellation of six satellites with medium noise instruments ($\sigma_{\mathrm{VEG50}} = 0.7$ ppm). The plumes were detected from (a) the CO_2 and (b) the NO_2 observations. The error bars show constant errors of $10.0\,\mathrm{Mt\,yr^{-1}}$ corresponding to the standard deviation of the differences between estimated and real emissions.

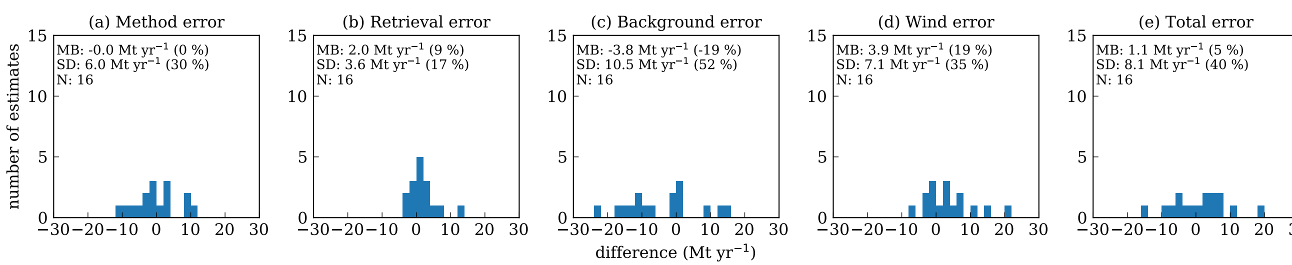

Figure S4. Histograms of (a) method, (b) retrieval, (c) background, (d) wind and (e) total errors for the emissions estimated by the mass-balance approach. The values are for plumes detected with the medium noise CO_2 observations ($\sigma_{\mathrm{VEG50}} = 0.7$ ppm) and line densities computed from the sub-polygon means.

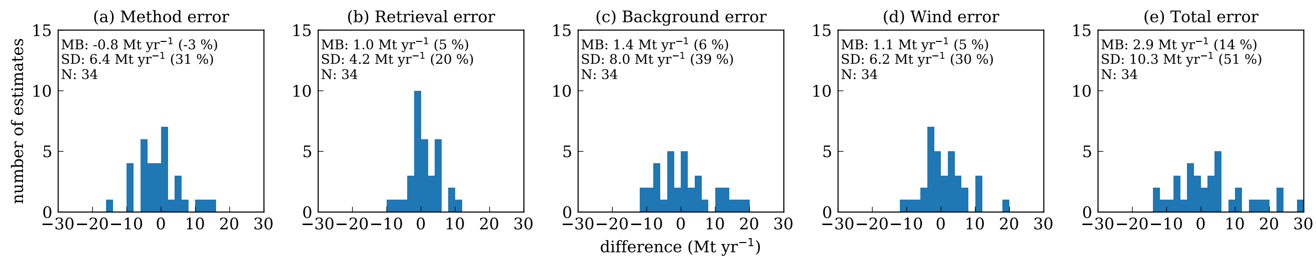

Figure S5. Same as Fig. S4 but for plumes detected from NO_2 observations.

S4 Additional tables

Table S1. Relative mean bias (MB in %), standard deviation (SD in %) and percentile range (PR in %) for method, retrieval, background, wind and total error using the CO_2 observations for detecting the plume. The percentile range was calculated between the 84th and 16th percentile and divided by two to make it comparable to the SDs.

	Method error			Retrieval error			Background error			Wind error			Total error		
σ_{VEG50} (ppm)	0.5	0.7	1.0	0.5	0.7	1.0	0.5	0.7	1.0	0.5	0.7	1.0	0.5	0.7	1.0
MB (sub-polygons)	4	-0	-1	7	10	13	-13	-19	-27	14	19	22	8	5	3
MB (Gauss)	7	4	3	13	17	14	-13	-12	-23	15	19	21	17	21	12
SD (sub-polygons)	32	30	33	17	18	22	57	53	49	39	35	35	47	40	45
SD (Gauss)	32	32	33	20	31	29	49	52	47	39	35	35	50	47	47
PR (sub-polygons)	34	30	36	11	11	22	62	51	41	26	29	33	53	33	41
PR (Gauss)	32	33	34	14	23	28	47	49	37	26	31	33	53	37	44

Table S2. Relative mean bias (MB in %), standard deviation (SD in %) and percentile range (PR in %) for method, retrieval, background, wind and total error using the NO_2 observations for detecting the plume. The percentile range was calculated between the 84th and 16th percentile and divided by two to make it comparable to the SDs.

	Method error			Retrieval error			Background error			Wind error			Total error		
σ_{VEG50} (ppm)	0.5	0.7	1.0	0.5	0.7	1.0	0.5	0.7	1.0	0.5	0.7	1.0	0.5	0.7	1.0
MB (sub-polygons)	-4	-4	-4	4	5	7	7	7	7	5	5	5	13	15	17
MB (Gauss CO2)	-3	-3	-3	5	8	17	13	14	16	6	6	6	22	26	31
MB (Gauss CO2+NO2)	-3	-3	1	5	9	14	13	15	14	6	6	3	18	22	25
SD (sub-polygons)	32	32	32	15	21	30	39	40	42	31	31	31	51	51	53
SD (Gauss CO2)	33	33	33	17	21	27	34	35	37	31	31	31	46	48	55
SD (Gauss CO2+NO2)	33	33	32	13	16	25	34	36	38	31	31	28	41	42	45
PR (sub-polygons)	24	24	24	13	18	26	44	46	46	23	23	23	54	51	46
PR (Gauss CO2)	29	29	29	15	21	28	37	38	35	26	26	26	37	38	40
PR (Gauss CO2+NO2)	29	29	29	11	16	24	37	38	35	26	26	28	41	40	43